ELSEVIER

International Journal of Thermal Sciences 41 (2002) 787–794

International Journal of Thermal Sciences

www.elsevier.com/locate/ijts

Effect of viscous dissipation on laminar mixed convection in a horizontal double-passage channel with uniform wall heat flux

M.M. Salah El-Din

P.O. Box 2574, Al-Sarai 21411, Alexandria, Egypt

Received 31 May 2001; accepted 18 September 2001

Abstract

The effect of viscous dissipation on fully developed laminar mixed convection in a horizontal double-passage channel has been investigated analytically. The channel is divided into two passages by means of a thin, perfectly conductive plane baffle and the walls have different uniform heat fluxes. Velocity and temperature profiles and the Nusselt number on the hot wall have been determined in closed forms. Results show that the Brinkman number has a significant effect on the dimensionless temperature, specially when the baffle is near to any of the channel's walls. The variations of the Nusselt number on the hot wall with Brinkman number depends on the baffle position.

Keywords: Horizontal channel; Laminar convection; Double-passage; Uniform heat flux; Viscous dissipation

1. Introduction

Laminar convection in horizontal channels has found applications in several different systems such as the cooling of electronic devices and the solar energy collection. This configuration has been the subject of several experimental and theoretical studies [1–18].

The convective heat transfer may be enhanced in a horizontal channel by using rough surface, inserts, swirl flow device, turbulent promoter, etc. [19]. Unfortunately, most of these methods cause a considerable drop in the pressure. Guo et al. [20] have suggested that the convective heat transfer could be enhanced by using special inserts. These inserts are designed to increase the included angle between the velocity vector and the temperature gradient vector, rather than to promote turbulence. So, the heat transfer is considerably enhanced with as little pressure drop as possible.

Cheng et al. [21] have studied the effect of a plane baffle, which is used as an insert, on the fully developed laminar convection in a horizontal channel. The authors have determined, in closed forms, the Nusselt number and temperature profiles for the channel under asymmetric heating. They have concluded that the presence of the baffle may lead to an enhancement of the heat transfer between the walls and fluid, according to the baffle position.

Cheng et al. have neglected the heat transfer due to the energy generated by viscous dissipation. Although viscous dissipation is usually neglected in low-speed and low-viscosity flows through conventionally sized channels of short lengths, it may become important when the length-to-width ratio is large [22]. For double-passage channels, the length-to-width ratio becomes large as the baffle becomes near the wall. So, viscous dissipation may become important.

In a previous work [23], the effect of viscous dissipation on fully developed combined convection in a horizontal double-passage channel with uniform symmetric and asymmetric wall temperatures has been investigated. The results showed that the increase in Brinkman number decreases the Nusselt number on the hot wall specially when the baffle becomes near it.

For the fully developed laminar duct flow, Guo et al. [20] observed that *Nu* for the case of the isoflux thermal boundary condition is greater than *Nu* for the case of isothermal boundary condition. This can be explained based on the concept of the included angle between the velocity and temperature gradient vectors. This angle is larger at isoflux thermal boundary condition than at isothermal boundary condition. Therefore, they stated that changing the thermal boundary condition could enhance the convective heat transfer. Therefore, the present work is devoted to study, analytically, the

E-mail address: msalaheldin@netscape.net (M.M. Salah El-Din).

1290-0729/02/$ – see front matter
PII: S1290-0729(02)01372-8

Nomenclature

b	channel width	m	
b^*	width of passage 1	m	
Br	Brinkman number $= \mu u_0^2/q_1 b$		
c_p	specific heat at constant pressure	$J\cdot kg^{-1}\cdot K^{-1}$	
h	heat transfer coefficient	$W\cdot m^{-2}\cdot K^{-1}$	
k	thermal conductivity	$W\cdot m^{-1}\cdot K^{-1}$	
Nu	Nusselt number $= hb/k$		
p	pressure	Pa	
q	heat flux	$W\cdot m^{-2}$	
R	heat flux ratio $= q_2/q_1$		
Re	Reynolds number $= u_0 b/\nu$		
T	temperature	K	
u	axial velocity	$m\cdot s^{-1}$	
x	axial coordinate	m	
y	transverse coordinate	m	
Y^*	$= b^*/b$		

Greek symbols

γ	pressure gradient	$Pa\cdot m^{-1}$
θ	dimensionless temperature	
μ	dynamic viscosity	$kg\cdot m^{-1}\cdot s^{-1}$
ν	kinematic viscosity	$m^2\cdot s^{-1}$
ρ	density	$kg\cdot m^{-3}$

Subscripts

b	bulk
c	cold wall plate
h	hot wall plate
0	reference
1	value in stream 1
2	value in stream 2

effect of viscous dissipation on fully developed combined convection in a horizontal double-passage channel with uniform wall heat flux.

2. Analysis

A physical configuration of the horizontal double-passage channel is shown in Fig. 1. The following assumptions are used in the analysis:

- The flow is laminar, two-dimensional, steady and fully developed.
- The fluid is incompressible and the physical properties are constants.
- The walls are kept at uniform heat fluxes.

With the above assumptions, the momentum equation is given by

$$\frac{\mathrm{d}^2 u_i}{\mathrm{d}y^2} = \frac{1}{\mu}\frac{\mathrm{d}p_i}{\mathrm{d}x} \tag{1}$$

where $i = 1$ refers to stream 1 and $i = 2$ stream 2.

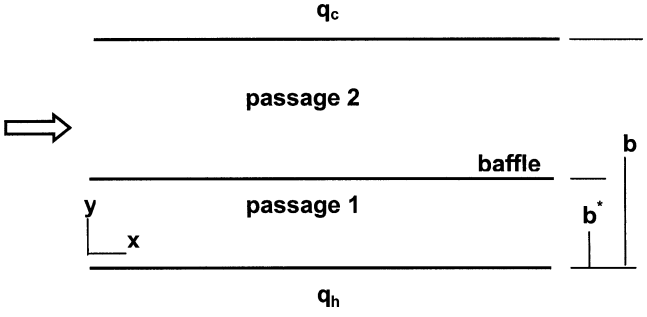

Fig. 1. Physical configuration of the horizontal double-passage channel.

The relevant boundary conditions are

$$y = 0: \quad u_1 = 0 \tag{2a}$$

$$y = b^*: \quad u_1 = u_2 = 0 \tag{2b}$$

$$y = b: \quad u_2 = 0 \tag{2c}$$

To make the momentum equation dimensionless, the following dimensionless quantities are introduced:

$$X = \frac{x}{b\,Re}, \qquad Y = \frac{y}{b}$$

$$U = \frac{u}{u_0}, \qquad P = \frac{p}{\rho u_0^2}, \qquad Re = \frac{u_0 b}{\nu}$$

where the reference velocity u_0 is defined as

$$u_0 = \frac{1}{b}\int_0^b u\,\mathrm{d}y \tag{3}$$

Hence, the dimensionless momentum equation is

$$\frac{\mathrm{d}^2 U_i}{\mathrm{d}Y^2} = \frac{\mathrm{d}P_i}{\mathrm{d}X} \tag{4}$$

The pressure gradient in Eq. (4) is assumed to be constant, i.e.,

$$\frac{\mathrm{d}P_i}{\mathrm{d}X} = \gamma_i \tag{5}$$

The dimensionless boundary conditions are

$$Y = 0: \quad U_1 = 0 \tag{6a}$$

$$Y = Y^*: \quad U_1 = U_2 = 0 \tag{6b}$$

$$Y = 1: \quad U_2 = 0 \tag{6c}$$

The solution to Eq. (4) gives

$$U_1 = \frac{\gamma_1}{2}\left(Y^2 - Y^* Y\right) \tag{7}$$

and

$$U_2 = \frac{\gamma_2}{2}\left[Y^2 - \left(1 + Y^*\right)Y + Y^*\right] \tag{8}$$

Conservation of mass considered at any cross section of the channel passages gives

$$\int_0^{Y^*} U_1 \,\mathrm{d}Y = Y^* \tag{9}$$

and

$$\int_{Y^*}^{1} U_2 \,\mathrm{d}Y = 1 - Y^* \tag{10}$$

Substitution from Eqs. (7) and (8) into Eqs. (9) and (10) gives the constants γ_1 and γ_2, i.e.,

$$\gamma_1 = -\frac{12}{Y^{*2}} \tag{11}$$

$$\gamma_2 = -\frac{12}{(1 - Y^*)^2} \tag{12}$$

Substitution from Eqs. (11) and (12) into Eqs. (7) and (8) leads to the following velocity profiles

$$U_1 = -\frac{6}{Y^{*2}}\left(Y^2 - Y^*Y\right) \tag{13}$$

and

$$U_2 = -\frac{6}{(1 - Y^*)^2}\left[Y^2 - \left(1 + Y^*\right)Y + Y^*\right] \tag{14}$$

The energy equation of the fully developed flow, taking into account the effect of viscous dissipation, is

$$k\frac{\partial^2 T}{\partial y^2} + \mu\left(\frac{\mathrm{d}u}{\mathrm{d}y}\right)^2 = \rho c_p u \frac{\partial T}{\partial x} \tag{15}$$

with boundary conditions

$$y = 0, \qquad \frac{\partial T}{\partial y} = -\frac{q_\mathrm{h}}{k} \tag{16a}$$

$$y = b^*, \qquad T_1 = T_2 \tag{16b}$$

$$y = b, \qquad \frac{\partial T}{\partial y} = \frac{q_\mathrm{c}}{k} \tag{16c}$$

Integration of Eq. (15) with respect to y in the interval $0 \to b$, using Eq. (3) yields

$$k\frac{\partial T}{\partial y}\bigg|_{y=b} - k\frac{\partial T}{\partial y}\bigg|_{y=0} + \mu\int_0^b \left(\frac{\mathrm{d}u}{\mathrm{d}y}\right)^2 \mathrm{d}y = \rho c_p u_0 b \frac{\partial T}{\partial x} \tag{17}$$

Using boundary conditions in Eq. (16), Eq. (17) takes the following form

$$\frac{\partial T}{\partial x} = \frac{1}{\rho c_p u_0 b}\left[q_\mathrm{h} + q_\mathrm{c} + \mu\int_0^b \left(\frac{\mathrm{d}u}{\mathrm{d}y}\right)^2 \mathrm{d}y\right] \tag{18}$$

Substitution from Eq. (18) into Eq. (15) gives the energy equation, which can be written in the following dimensionless from

$$\frac{\partial^2\theta}{\partial Y^2} + Br\left(\frac{\mathrm{d}U}{\mathrm{d}Y}\right)^2 = \left[1 + R + Br\int_0^1 \left(\frac{\mathrm{d}U}{\mathrm{d}Y}\right)^2 \mathrm{d}Y\right]U \tag{19}$$

where

$$\theta = \frac{T - T_0}{q_\mathrm{h} b/k}, \qquad Br = \frac{\mu u_0^2}{q_\mathrm{h} b}, \qquad R = \frac{q_\mathrm{c}}{q_\mathrm{h}}$$

The reference temperature T_0 is defined as

$$T_0 = \frac{1}{b}\int_0^b T \,\mathrm{d}y \tag{20}$$

The dimensionless boundary conditions are

$$Y = 0, \qquad \frac{\partial\theta}{\partial Y} = -1 \tag{21a}$$

$$Y = Y^*, \qquad \theta_1 = \theta_2 \tag{21b}$$

$$Y = 1, \qquad \frac{\partial\theta}{\partial Y} = R \tag{21c}$$

By differentiation of Eqs. (13) and (14) with respect to y, the term $(\frac{\mathrm{d}U}{\mathrm{d}Y})^2$ in Eq. (19) can be obtained and as a consequence, the integration in the right-hand side can be evaluated.

$$\int_0^1 \left(\frac{\mathrm{d}U}{\mathrm{d}Y}\right)^2 \mathrm{d}Y = \int_0^{Y^*} \left(\frac{\mathrm{d}U_1}{\mathrm{d}Y}\right)^2 \mathrm{d}Y + \int_{Y^*}^1 \left(\frac{\mathrm{d}U_2}{\mathrm{d}Y}\right)^2 \mathrm{d}Y = \frac{12}{Y^*(1 - Y^*)} \tag{22}$$

So, Eq. (19) can be rewritten as

$$\frac{\partial^2\theta}{\partial Y^2} + Br\left(\frac{\mathrm{d}U}{\mathrm{d}Y}\right)^2 = ZU \tag{23}$$

where

$$Z = 1 + R + \frac{12\,Br}{Y^*(1 - Y^*)} \tag{24}$$

Integration of Eq. (23) twice with respect to Y for the two passages of the channel, using Eq. (21), gives

$$\theta_1 = \left(\frac{24\,Br}{Y^{*2}} + Z\right)\left(\frac{-1}{2Y^{*2}}Y^4 + \frac{1}{Y^*}Y^3\right) - \frac{18\,Br}{Y^{*2}}Y^2 - Y + F_1 \tag{25}$$

$$\theta_2 = \frac{-1}{(1 - Y^*)^2}\left[\frac{24\,Br}{(1 - Y^*)^2} + Z\right]\left[\frac{1}{2}Y^4 - \left(1 + Y^*\right)Y^3\right] - \frac{3}{(1 - Y^*)^2}\left[\frac{6\,Br(1 + Y^*)^2}{(1 - Y^*)^2} + ZY^*\right]Y^2 + G_1 Y + G_2 \tag{26}$$

The constant G_1 is given by

$$G_1 = R - \frac{1+3Y^*}{(1-Y^*)^2}\left[\frac{24\,Br}{(1-Y^*)^2} + Z\right] + \frac{6}{(1-Y^*)^2}\left[\frac{6\,Br(1+Y^*)^2}{(1-Y^*)^2} + ZY^*\right] \quad (27)$$

Substitution from Eqs. (25) and (26) into Eq. (21b) gives the following relation

$$G_2 = G_3 + F_1 \quad (28)$$

where

$$G_3 = \frac{Y^{*2}}{2}\left(\frac{24\,Br}{Y^{*2}} + Z\right) - 18\,Br - Y^* - \frac{(1+Y^*/2)Y^{*3}}{(1-Y^*)^2}\left[\frac{24\,Br}{(1-Y^*)^2} + Z\right] + \frac{3Y^{*2}}{(1-Y^*)^2}\left[\frac{6\,Br(1+Y^*)^2}{(1-Y^*)^2} + ZY^*\right] - G_1Y^* \quad (29)$$

The constant F_1 can be obtained by use of Eq. (20). Introducing the dimensionless parameters into Eq. (20) gives

$$\int_0^1 \theta\,dY = 0 \quad (30)$$

Thus

$$\int_0^{Y^*} \theta_1\,dY + \int_{Y^*}^1 \theta_2\,dY = 0 \quad (31)$$

Integration of Eq. (25) with respect to Y in the interval $0 \to Y^*$ gives

$$\int_0^{Y^*} \theta_1\,dY = F_1Y^* + F_2 \quad (32)$$

where

$$F_2 = \frac{Y^*}{20}\left(3ZY^{*2} - 10Y^* - 48\,Br\right) \quad (33)$$

Integration of Eq. (26) with respect to Y in the interval $Y^* \to 1$ gives

$$\int_{Y^*}^1 \theta_2\,dY = F_1\left(1-Y^*\right) + G_4 \quad (34)$$

where

$$G_4 = \frac{-1}{(1-Y^*)^2}\left[\frac{1-Y^{*5}}{10} - \frac{(1+Y^*)(1-Y^{*4})}{4}\right] \times \left[\frac{24\,Br}{(1-Y^*)^2} + Z\right] - \frac{1-Y^{*3}}{(1-Y^*)^2}\left[\frac{6\,Br(1+Y^*)^2}{(1-Y^*)^2} + ZY^*\right] + \frac{G_1}{2}\left(1-Y^{*2}\right) + G_3\left(1-Y^*\right) \quad (35)$$

Adding Eq. (32) to Eq. (34) gives the constant F_1

$$F_1 = -(F_2 + G_4) \quad (36)$$

The Nusselt number for the hot wall is

$$Nu_h = \frac{1}{\theta_h - \theta_{b1}} \quad (37)$$

The dimensionless bulk temperature for passage 1 is defined as

$$\theta_{b1} = \int_0^{Y^*} U_1\theta_1\,dY \Big/ \int_0^{Y^*} U_1\,dY = \int_0^{Y^*} U_1\theta_1\,dY/Y^* \quad (38)$$

3. Results and discussions

Solutions to the energy equation show that the temperature profiles depend on three parameters. They are the ratio of heat fluxes, the Brinkman number and the baffle position. Solutions to the momentum equation show that the velocity profiles are functions of the baffle position only. In the following sections the effect of Brinkman number on the Nusselt number on the hot wall and temperature profiles through the channel will be presented at different positions of the baffle with symmetric ($R = 1$) and asymmetric ($R \neq 1$) heating. Four cases of asymmetric heating will be considered: fluid heating at both walls ($R = 0.5$), the upper wall is adiabatic ($R = 0$), fluid heating at the lower wall and fluid cooling at the upper wall ($R = -0.5, -1$).

3.1. Symmetric heating

Fig. 2 presents the effect of Br on the temperature profiles for the case of symmetric heating at different positions of the baffle. The figure reveals that an increase in Br increases the temperature significantly in the narrower passage. This is due to the increasing in viscous heating since the length-to-width ratio is large in the narrower passage. This increasing in temperature in the narrower passage is accompanied with a significant decrease in temperature next to the wall of the wider passage. This can be explained with the aid of Eq. (30) which implies that the integration of the temperature through the whole channel is zero. When the baffle is in the middle of the channel, equal effects of viscous dissipation are attained in the two passages. As a consequence, the temperature increases next to both walls of the channel and an axis of symmetry exists in the middle of the channel. The figure reveals also that at certain values of Y, Br has no effect on the dimensionless temperature. Mathematically, this occurs when the terms including the Brinkman number in Eqs. (25) and (26) vanish.

Table 1 presents the variations of Nu_h with Br at different positions of the baffle for symmetric heating. The table shows that for $Y^* \leqslant 0.5$, Nu_h is a decreasing function of Br. This can be explained with the aid of Fig. 2 which shows that for $Y^* \leqslant 0.5$, θ_h is an increasing function of Br. So,

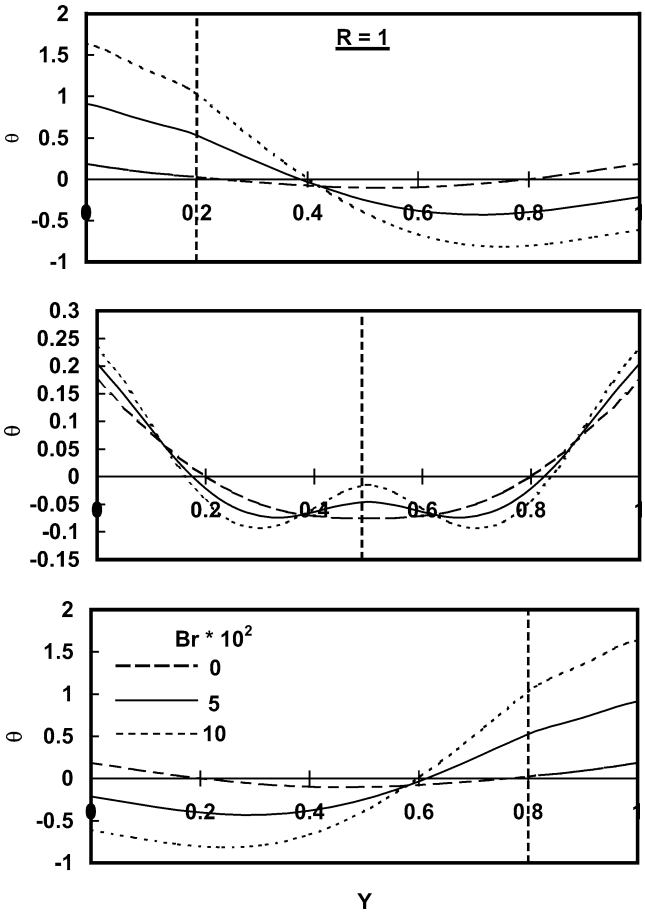

Fig. 2. Effect of *Br* on temperature profiles for symmetric heating.

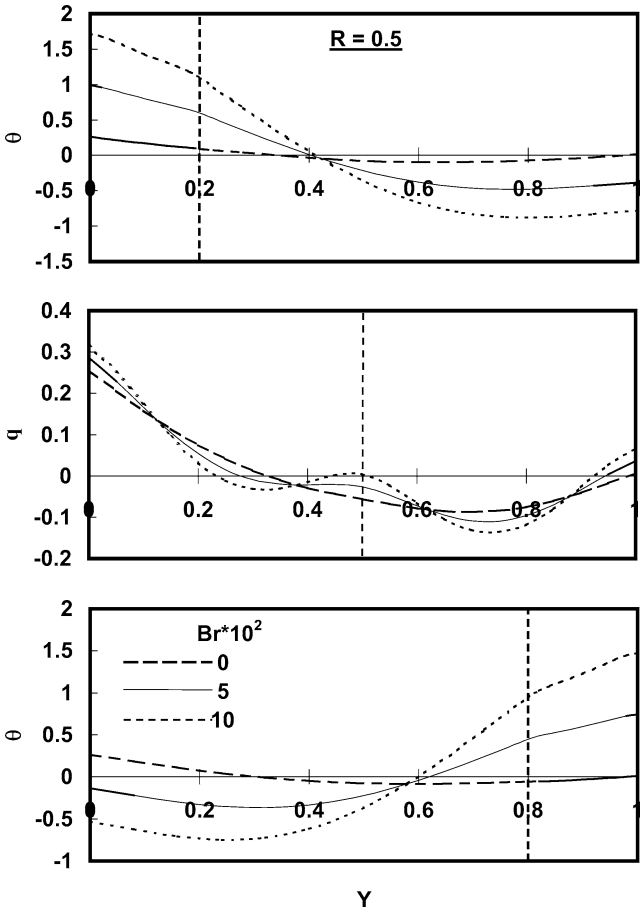

Fig. 3. Effect of *Br* on temperature profiles for asymmetric heating with $R = 0.5$.

Table 1
Variations of Nu_h with *Br* at different positions of the baffle for symmetric heating

$Br \times 10^2$	Nu_h		
	$Y^* = 0.2$	$Y^* = 0.5$	$Y^* = 0.8$
0	11.147	5.385	4.248
1	9.174	5.17	5.08
2	7.795	4.972	6.318
3	6.776	4.788	8.353
4	5.993	4.617	12.324
5	5.372	4.459	23.49
6	4.868	4.31	250
7	4.45	4.172	−28.925
8	4.098	4.042	−13.672
9	3.798	3.919	−8.951
10	3.539	3.804	−6.654

the denominator of Eq. (37) increases and as a consequence, Nu_h decreases. Table 1 shows also that the rate of decreasing in Nu_h, due to the increasing in *Br*, increases as the baffle is nearer to the hot wall. As mentioned before, this is because of the increasing of the effect of viscous dissipation as the length-to-width ratio becomes large. Also, it may be noted that at a given value of *Br*, Nu_h increases as the baffle is nearer to the hot wall. This is due to the increase in the included angle between the velocity vector and the temperature gradient vector. For large values of *Br*, viscous dissipation is more effective on the Nusselt number than the included angle between the velocity vector and the temperature gradient vector. Therefore, Nu_h decreases as the baffle is nearer to the hot wall. For example, see Table 1 at $Br = 0.1$.

When the baffle is nearer to the upper wall, Nusselt number on the lower wall increases up to a very high value as *Br* increases. With more increasing in *Br*, Nu_h changes its sign. Fig. 2 shows that the dimensionless temperature on the wall from which the baffle is far is a decreasing function of *Br*. So, the difference between the wall temperature and the bulk temperature in the denominator of Eq. (37) becomes very small and as a consequence, the value of Nu_h becomes very high. More increasing in *Br* makes the denominator of Eq. (37) negative and as a consequence, Nu_h changes its sign.

3.2. Asymmetric heating

The effects of *Br* on the temperature profiles at different positions of the baffle for the four cases of asymmetric heating are shown in Figs. 3–6. For $Br = 0$, the temperature

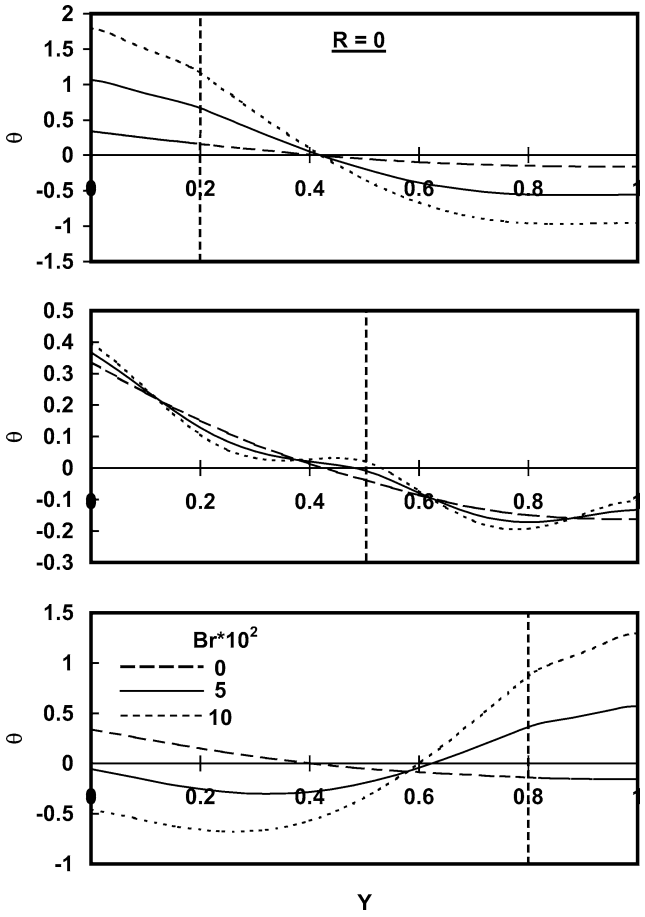

Fig. 4. Effect of *Br* on temperature profiles for asymmetric heating with $R = 0$.

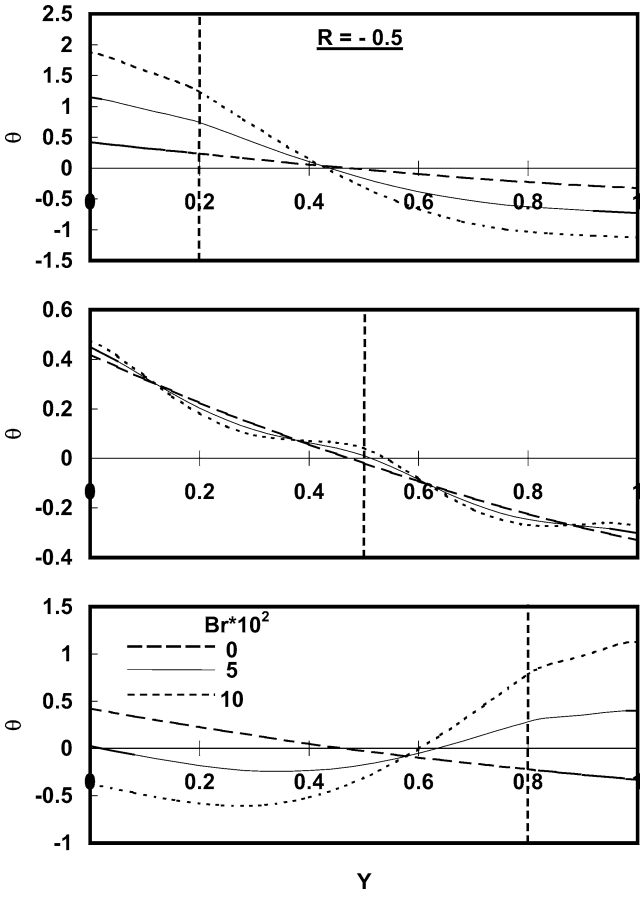

Fig. 5. Effect of *Br* on temperature profiles for asymmetric heating with $R = -0.5$.

Table 2
Variations of Nu_h with *Br* at different positions of the baffle for asymmetric heating with $R = 0.5$

$Br \times 10^2$	Nu_h		
	$Y^* = 0.2$	$Y^* = 0.5$	$Y^* = 0.8$
0	10.836	4.956	3.616
1	8.963	4.773	4.202
2	7.642	4.604	5.014
3	6.66	4.446	6.217
4	5.902	4.298	8.178
5	5.299	4.16	11.945
6	4.808	4.031	22.152
7	4.4	3.91	152.172
8	4.056	3.795	−31.25
9	3.761	3.687	−14.17
10	3.507	3.585	−9.162

Table 3
Variations of Nu_h with *Br* at different positions of the baffle for asymmetric heating with $R = 0$

$Br \times 10^2$	Nu_h		
	$Y^* = 0.2$	$Y^* = 0.5$	$Y^* = 0.8$
0	10.542	4.59	3.147
1	8.761	4.433	3.582
2	7.495	4.287	4.157
3	6.548	4.149	4.95
4	5.814	4.021	6.119
5	5.228	3.9	8.009
6	4.749	3.786	11.589
7	4.351	3.678	20.958
8	4.014	3.577	109.375
9	3.725	3.481	−33.981
10	3.476	3.39	−14.706

on the hot wall is greater than that on the cool wall because the heat flux on the hot wall is greater than that on the cool wall. For $Br > 0$, the effect of viscous dissipation on the temperature profiles is similar to that for the case of symmetric heating. For $R = -1$ with $Br = 0$, the temperature varies linearly with Y as for the case of uniform wall temperatures.

The variations of Nu_h with *Br* are presented in Table 2 for $R = 0.5$ at different positions of the baffle. From the table it is evident that Nu_h varies with *Br* in a manner similar to that for the case of symmetric heating except that the change in sign of Nu_h at $Y^* = 0.8$ occurs at higher value of *Br* than that for symmetric heating. As mentioned before, this is due to that the heat flux on the hot wall is greater than that on the cool wall.

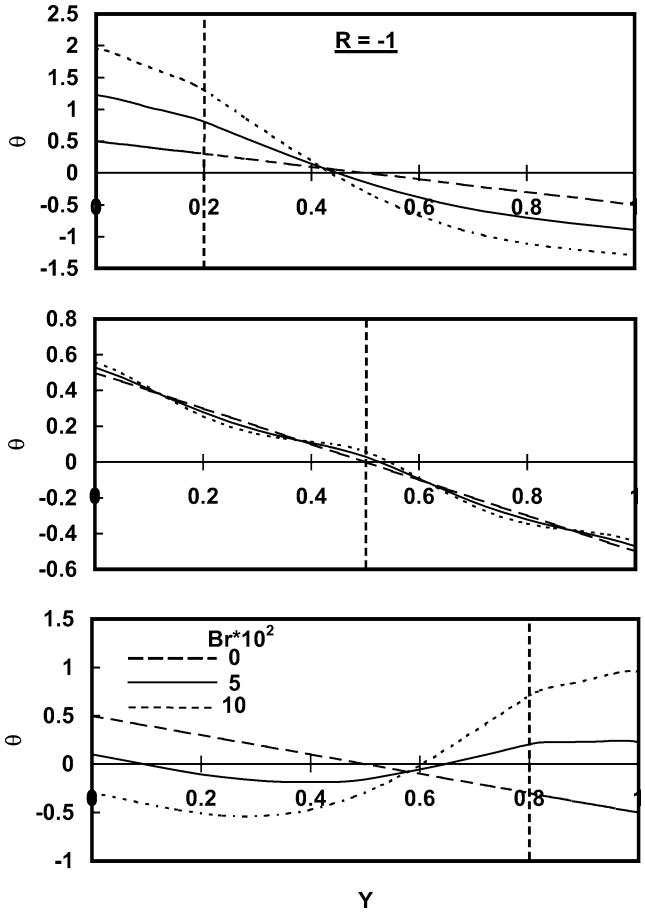

Fig. 6. Effect of *Br* on temperature profiles for asymmetric heating with $R = -1$.

Table 4
Variations of Nu_h with *Br* at different positions of the baffle for asymmetric heating with $R = -0.5$

$Br \times 10^2$	Nu_h		
	$Y^* = 0.2$	$Y^* = 0.5$	$Y^* = 0.8$
0	10.264	4.275	2.787
1	8.568	4.138	3.122
2	7.353	4.01	3.55
3	6.44	3.89	4.113
4	5.728	3.777	4.888
5	5.158	3.67	6.024
6	4.692	3.569	7.848
7	4.302	3.473	11.254
8	3.973	3.382	19.886
9	3.69	3.296	85.366
10	3.445	3.215	−37.234

Table 5
Variations of Nu_h with *Br* at different positions of the baffle for asymmetric heating with $R = -1$

$Br \times 10^2$	Nu_h		
	$Y^* = 0.2$	$Y^* = 0.5$	$Y^* = 0.8$
0	10	4	2.5
1	8.383	3.88	2.767
2	7.216	3.767	3.097
3	6.335	3.661	3.518
4	5.645	3.561	4.07
5	5.091	3.465	4.828
6	4.636	3.375	5.932
7	4.255	3.289	7.692
8	3.933	3.208	10.938
9	3.655	3.131	18.919
10	3.415	3.057	70

When the upper wall is insulated ($R = 0$), more viscous heating is required to change the sign of Nu_h at $Y^* = 0.8$ as shown in Table 3. Table 3 shows also that Nu_h at $Y^* = 0.2$ is always greater than Nu_h at $Y^* = 0.5$ for all given values of *Br*. This is because of the increasing in the dimensionless temperature on the hot wall.

Table 4 presents the variations of Nu_h with *Br* at different positions of the baffle for the case of fluid heating at the lower wall and fluid cooling at the upper wall ($R = -0.5$). The table shows that Nu_h still change its sign at $Y^* = 0.8$ but at a greater value of *Br* than that for the previous cases. Table 5 shows that up to a Brinkman number value of 0.1 no change in the sign of Nu_h occurs at $Y^* = 0.8$.

4. Conclusion

An analytical solution for laminar mixed convection with viscous dissipation in a horizontal double-passage channel has been developed in the fully developed region. Uniform wall heat fluxes with symmetric and asymmetric heating have been considered. The temperature profiles have been presented and the Nusselt number on the hot wall has been evaluated at different positions of the baffle. It can be concluded that:

(1) Brinkman number has no effect on the velocity profiles which are functions of the baffle position only.
(2) An increase in Brinkman number leads to a significant increase in the dimensionless temperature in the narrower passage for both symmetric and asymmetric heating. This is accompanied with a significant decrease in the dimensionless temperature in the wider passage.
(3) When the baffle is in the middle of the channel the effect of Brinkman number on the dimensionless temperature in the whole channel decreases clearly, specially for negative *R*.
(4) For $Y^* \leqslant 0.5$, the Nusselt number on the hot wall is a decreasing function of Brinkman number.
(5) When the baffle is far from the hot wall Nu_h becomes an increasing function of Brinkman number. At a certain value of Brinkman number Nu_h changes its sign. For symmetric heating this change in sign of Nu_h occurs at less value of *Br* than that for asymmetric heating.
(6) For $R > 0$ with large values of Brinkman number, Nu_h decreases as the baffle is nearer to the hot wall. For

$R \leqslant 0$, this behavior disappears for all given values of Brinkman number.

References

[1] C. Gau, C.W. Liu, T.M. Huang, W. Aung, Secondary flow and enhancement of heat transfer in horizontal parallel-plate and convergent channels heating from below, Inter. J. Heat Mass Transfer 42 (1999) 2629–2647.

[2] D.B. Ingham, P. Watson, P.J. Heggs, Upstream migration of heat during combined convection in a horizontal parallel plate duct, Internat. J. Heat Mass Transfer 39 (1996) 437–440.

[3] W.L. Lin, T.F. Lin, Experimental study of unstable mixed convection of air in a bottom heated horizontal rectangular duct, Internat. J. Heat Mass Transfer 39 (1996) 1649–1663.

[4] D.B. Ingham, P. Watson, P.J. Heggs, Recirculating laminar mixed convection in a horizontal parallel plate duct, Internat. J. Heat Fluid Flow 16 (1995) 202–210.

[5] C.C. Huang, T.F. Lin, Buoyancy induced flow transition in mixed flow of air through a bottom heated horizontal rectangular duct, Internat. J. Heat Mass Transfer 37 (1994) 1235–1255.

[6] T.A. Nyce, J. Ouazzani, A. Durand-Daubin, F. Rosenberger, Mixed convection in a horizontal rectangular channel-experimental and numerical velocity distributions, Internat. J. Heat Mass Transfer 35 (1992) 1481–1494.

[7] F.C. Chou, W.Y. Lien, Effect of wall heat conduction on laminar mixed convection in the thermal entrance region of horizontal rectangular channels, Wärme- und Stoffübertragung 26 (1991) 121–127.

[8] F.S. Lee, G.J. Hwang, Transient analysis on the onset of thermal instability in the thermal entrance region of a horizontal parallel plate channel, J. Heat Transfer 113 (1991) 363–370.

[9] J.R. Maughan, F.P. Incropera, Fully developed mixed convection in a horizontal channel heated uniformly from above and below, Numer. Heat Transfer 17 (1990) 417–430.

[10] F.P. Incropera, A.L. Knox, J.R. Maughan, Effect of wall heat flux distribution on laminar mixed convection in the entry region of a horizontal rectangular duct, Numer. Heat Transfer 13 (1988) 427–450.

[11] H.V. Mahaney, F.P. Incropera, S. Ramadhyani, Development of laminar mixed convection flow in a horizontal rectangular duct with uniform bottom heating, Numer. Heat Transfer 12 (1987) 137–155.

[12] F.C. Chou, G.J. Hwang, Vorticity-velocity method for Graetz problem with the effect of natural convection in a horizontal rectangular channel with uniform wall heat flux, J. Heat Transfer 109 (1987) 704–710.

[13] F.P. Incropera, J.A. Schutt, Numerical simulation of laminar mixed convection in the entrance region of horizontal rectangular ducts, Numer. Heat Transfer 8 (1985) 707–729.

[14] D.G. Osborne, F.P. Incropera, Laminar, mixed convection heat transfer for flow between horizontal parallel plates with asymmetric heating, Internat. J. Heat Mass Transfer 28 (1985) 207–217.

[15] K.J. Kennedy, A. Zebib, Combined free and forced convection between horizontal parallel planes: Some case studies, Internat. J. Heat Mass Transfer 26 (1983) 471–478.

[16] M.M.M. Abou-Ellail, S.M. Morcos, Buoyancy effects in the entrance region of horizontal rectangular channels, J. Heat Transfer 105 (1983) 924–928.

[17] K.C. Cheng, S.W. Hong, G.J. Hwang, Buoyancy effects on laminar heat transfer in the entrance region of horizontal rectangular channels with uniform wall heat flux for large Prandtl number fluids, Internat. J. Heat Mass Transfer 15 (1972) 1819–1836.

[18] K.C. Cheng, G.J. Hwang, Numerical solution for combined free and forced laminar convection in horizontal rectangular channels, J. Heat Transfer 91 (1969) 59–66.

[19] R.L. Webb, Principles of Enhanced Heat Transfer, Hemisphere, Washington, DC, 1995.

[20] Z.Y. Guo, D.Y. Li, B.X. Wang, A novel concept for convective heat transfer enhancement, Internat. J. Heat Mass Transfer 41 (1998) 2221–2225.

[21] C.H. Cheng, H.S. Kou, W.H. Hwang, Laminar fully developed forced convection flow within an asymmetrically heated horizontal double-passage channel, Appl. Energy 33 (1989) 265–286.

[22] C.P. Tso, S.P. Mahulikar, The use of the Brinkman number for single phase forced convective heat transfer in microchannels, Internat. J. Heat Mass Transfer 41 (1998) 1759–1769.

[23] M.M. Salah El-Din, Effect of viscous dissipation on fully developed combined convection in a horizontal double-passage channel, Heat Mass Transfer, in press.